

Performance analysis of ice storage air conditioning system driven by distributed photovoltaic energy

Y. F. Xu^{1,2}, M. Li^{1,*}, X. Luo¹, Y. F. Wang¹, Q. F. Yu¹, R. H. E. Hassaniem^{1,3}

¹ Solar Energy research Institute, Yunnan Normal University, Kunming, Yunnan 650500, China

² Zhejiang Solar Energy Product Quality Inspection Center, Haining, Zhejiang 314416, China

³ Agricultural Engineering Department, Faculty of Agriculture, Cairo University, Cairo 12613, Egypt

In this paper, an ice storage air conditioning system (ISACS) driven by distributed photovoltaic energy system (DPES) was proposed. Furthermore, the system structure optimization analysis was also investigated. The energy coupling and transferring characteristics in light-electricity-cold conversion process were analysed by the theoretical calculations and experimental tests. Results revealed that the system energy utilization efficiency and exergy efficiency were 4.64% and 43.91%, respectively. The energy losses were high in photo-electric conversion process and the ice making process of ice slide machine. Therefore, the immersed evaporator and co-integrated exchanger were adopted and the ice making efficiency and solar energy utilization ratio were improved with the increasing of the system energy efficiency.

Keywords: photovoltaic, ice storage, energy, exergy, structure optimization

INTRODUCTION

With the dramatic climate changes, the cooling demand has been increased and led to a rapid growth of energy consumption, which causes traditional fossil fuel energy shortage and great damage to climate and environment with the emissions of CO₂ and harmful particles by extensive use of traditional fossil energy. Furthermore, using the electric air conditioning increases the electrical pressure in the peak time and increases the tense situation between power supply and demands. Therefore, refrigeration driven by solar energy becomes one of the promising approaches to reduce or partially replace the conventional refrigeration systems. There are two main working modes of solar refrigeration namely, solar thermal refrigeration and solar photovoltaic refrigeration [1, 2]. Several studies have been conducted about different solar refrigeration options in the last years for the improvement and development of solar thermal refrigeration system such as operation efficiency and operating stability [3-11]. Solar photovoltaic (PV) refrigeration has more advantages on refrigerating effect, stable operation and energy utilization rate compared to solar thermal refrigeration. The cost of PV module decreased by 75% from 2009 to 2014 all over the world and the cost of average electricity of large-scale photovoltaic power plant has been cut in half from 0.30 dollar/kWh in 2010 down to 0.15 dollar/ kWh

in 2014; furthermore the reduction was more than 60% for distributed photovoltaic power plant. At the same time, the photoelectric conversion efficiency of PV module increased year by year and the efficiencies of poly-silicon PV module and single crystal silicon PV module were improved to 18.7% and 20.4% in 2015, respectively. Household refrigeration system, driven by distributed photovoltaic energy system (DPES), has been developed rapidly with PV investment by decreasing its operation cost and improving the conversion efficiency of PV module.

Axaopoulos et al. [12] designed a PV Ice-maker without battery and studied its performance when the compressor operating efficiency was 9.2%, they found that this prototype have a good ice-making capability and reliable operation as well as a great improvement in the start up characteristics of the compressors, which remain working even during days with low solar irradiation of 150 W/m². It was also reported that the required photovoltaic panel area of a solar electric-vapor compression refrigeration system increases as the evaporating temperature decreases and the coefficient of performance variation of the cooling system decreases with the decreasing of evaporating temperature [13]. Ekren et al. [14] studied the photovoltaic DC refrigerator system and found that PV module conversion efficiency has a greater impact on the system exergy efficiency. Aktacir [15] designed a multifunctional PV refrigerator and found that when indoor and outdoor average temperatures were 26.3 °C and 24.9 °C, the minimum temperature of the

* To whom all correspondence should be sent:
lmllldy@126.com

10.6 °C. Mba et al. [16] used MATLAB software to simulate PV refrigeration system operating process and analysis system operating characteristics in different conditions. Furthermore, Tina et al.[17] designed a software for monitoring and managing stand-alone PV refrigerator system in a remote area, which had a real-time monitor running status and automatically recorded data feeding back to the terminal equipment. In addition, Kaplanis et al.[18] improved the performance of a traditional refrigerator which driven by PV. The energy conversion, management and operation performance for PV refrigerator system powered on three conditions such as, photovoltaic components, battery and outage showed that the system COP gradually decreases from morning till night [19]. The American SOLUS Refrigeration Company has developed a photovoltaic DC refrigerator substituting battery with water-propylene/ethylene glycol phase change material to store cold and reduce the system investing and running cost. Results revealed that the temperature inside the refrigerator was remaining stable at around 1.4 °C when the environment temperature was 32 °C. Recently, the PV refrigeration system has been improved and developed in the aspects of product structure, operating efficiency and refrigeration performance. According to comprehensive analysis, PV refrigeration system research is currently mainly concentrated on ice maker driven by PV. Batteries are essential component to store energy and to solve the intermittent of solar energy in PV refrigeration system. However, batteries increase the investing and running costs and reduce the system energy conversion and utilization ratios. Thus, ice storage technology has attracted researcher's attention. Ice storage technology has a great role on saving building energy, transfer peak power to off-peak, improve grid load rate and others aspects. It is clear that in the tropical regions, such as Xishuang banna in China and Bangkok in Thailand, have almost 300 days for cooling demand thereby, ice storage has a good application prospect in those regions.

Thus, ice storage air conditioning system (ISACS) driven by distributed photovoltaic energy system (DPES) was established based on our previous research results [20]. A few batteries were used in order to provide the stability for system operation. At first, a theoretical model has been established and experimental work has been implemented to analyze the energy coupling and transferring characteristics in light-electricity-cold

conversion process. And then, the system structure optimization analysis was also investigated for a higher energy utilization efficiency and better financial rewards.

MATERIALS AND METHODS

Configuration of ISACS driven by DPES

The ice storage air conditioning system (ISACS) of 0.2 kW driven by distributed photovoltaic energy system (DPES) was mainly configured by DPES, ice maker, cold storage system and air conditioning system. The pictures of ISACS driven by DPES are shown in Fig.1.



Fig.1. Pictures of a 0.2 kW ISACS driven by DPES

PV modules converts solar energy into electric energy which can be regulated by controller with maximum power point tracking (MPPT) to drive ice maker, ice storage system and air conditioning system. The MPPT device adopted in the controller is mainly composed of single chip microcomputer and photovoltaic power control unit and there were PWM driver, the empirical formula calculation unit, boots circuit and many other components in PV power control unit contains. The algorithm of MPPT control device, combined with the engineering mathematical model of PV modules and the two interpolation method, was employed to achieve maximum power point tracking. In daytime, DPES receives solar energy and turns it into direct-current (DC) electric power which can be converted to alternating current (AC) electric power by inverter to drive AC compressor, water pump, ethylene glycol pump and fan coil. In order to maintain the stability of electric energy supply, a few batteries were adopted and connected with controller to maintain the energy conversion and supply in the most optimized way. Ice maker and storage system was made up with AC compressor, condenser, expansion valve, disc evaporator and

ice storage tank. Circulating water can be frozen in the disc evaporator and then the ice droop into ice storage tank. Thereby, the ice maker worked as vapour compression refrigeration. In the AC compressor, the cryogenic R134a was compressed at a high temperature and high pressure gas to be filtered in gas-liquid separator and to release heat in condenser. Refrigerant was condensed to mild temperature and high pressure gas. When the gas inflows into throttle valve, it can be throttled to low temperature and low pressure liquid then feeds into plat evaporator. Subsequently, flows out of the evaporator, the refrigerant flows into the other gas-liquid separator to be sucked into the compressor. Finally, the refrigeration cycle will be completed. Air conditioning system was mainly made up of coil heat exchanger which was fixed in ice storage tank, Ethylene glycol pump, solenoid valve, proportional control valve and fan coil. Ethylene glycol was employed as a cold exchanging medium. All connecting pipes were wrapped with rubber insulation material and the ice storage tank was covered with polyurethane foam insulation.

The main components and parameters of ISACS driven by DPES are shown in Table 1.

Table 1. Main components and parameters of ISACS driven by DPES

Components	Parameters
PV module	P_m : 245 W, V_m : 34.5 V, I_m : 7.10 A, V_{OC} : 43.5 V, I_{SC} : 8.18 A, module: length*wide: 1640 mm*990 mm, cells in series: length*wide*numbers: 155 mm*155 mm*60.
Controller	12-48 V 60 A charge, 30 A load
Inverter	P : 3 kW, DC input voltage: 48 V, output voltage: 220 V, output frequency: 50 Hz.
Batteries	Battery capacity: 12 V65 Ah, four batteries in series
Refrigerant	Molecular formula: CH_2FCF_3 , boiling point: $-26.1\text{ }^\circ\text{C}$, critical temperature: $101.1\text{ }^\circ\text{C}$.
Ice maker	Ice production: 2.08 kg/h, P : 380 W.
Ice storage tank	Capacity: 20 cm*20 cm*20 cm
Cold exchanging medium	Melting point: $-12.6\text{ }^\circ\text{C}$, viscosity: 25.66 mPa s.
Pump	Power: 46-93 W, life: 6 m, maximum flow rate: 3.4 m ³ /h.
Fan coil	Fan type: YS 56-2, power: 180 W, voltage: 380 V, Current: 0.53 A, speed: 2800 r/min, number of fins: 95, size: 23 cm*8 cm*20 cm, coil numbers: 26, Coil inner diameter: 6 mm.

DPES were made up of two 245 W_p polycrystalline silicon PV modules in series and four valve controlled sealed maintenance free lead-acid batteries in series were used to maintain the stability of system operation. Refrigerant (R134a) temperature and pressure were measured by T-type thermocouples and pressure transducers, respectively. Voltages and currents of PV modules were measured by a digital multimeter. The wind speed was measured by the wind speed transducer. Solar irradiation was measured by pyranometer. The compressor input power was measured by a wattmeter. Electromagnetic flow meter was used to measure refrigerant flow and cold exchanging medium flow. The parameters of all instruments are shown in Table 2.

Table 2. The instruments parameters

Instrument	Parameters and accuracy
Digital multimeter	FLUKE F-179, DC voltage measurement accuracy: $\pm 0.9\%+2$, DC current value measurement accuracy: $\pm 1\%+3$.
Thermocouples	Type: T, range: -200 to $350\text{ }^\circ\text{C}$, accuracy: $\pm 0.4\%$ of full scale
Wind speed transducer	EC-9S, range: 0-70 m/s, accuracy: ± 0.3 m/s, resolution ratio: 0.1 m/s
Electromagnetic flow meter	SIEMENS FUP 1010, range: -12 m/s~ 12 m/s, accuracy: <0.3 m/s (1 ft/s), $\pm 0.5\% \sim \pm 2.0\%$,
Electronic balance	AHW-3, range: 0-3 kg, accuracy: ± 0.05 g
Pressure transducer	Range: 0-0.6 MPa low side and 0-1.8 MPa high side accuracy: $\pm 0.25\%$ of full scale at $25\text{ }^\circ\text{C}$
Pyranometer	Kipp & zonen CMP6, Range: 0-2000 W/m ² , accuracy: $\pm 5\%$
Wattmeter	DELIXI DDS607, Type: 220 V 20 A 50 Hz 3200 imp/kW, accuracy: 0.01 kW h
Data acquisition unit	Agilent 34972A data acquisition unit

The theoretical models of energy conversion and transfer characteristics of ISACS driven by DPES

The theoretical model was established to analyze the energy conversion and transfer characteristics of ISACS driven by DPES as follow.

(1) Theoretical models of DPES

Transient energy balance equation of PV modules is expressed as:

$$Q_{pv,in} = S_p m C_p \frac{dT_p}{dt} + Q_{pv,rad} + Q_{pv,conv} + Q_{pv,elect} \quad (1)$$

The solar energy which absorbed by PV modules can be estimated as:

$$Q_{pv,in} = \alpha \tau G S_p \quad (2)$$

Radiation heat loss can be given by:

$$Q_{pv,rad} = S_p F_{ps} \sigma (\varepsilon_p T_p^4 - \varepsilon_s T_s^4) \quad (3)$$

T_s is the sky temperature (K), which is 0.914 times of ambient temperature suggested by [21].

Convective heat loss can be estimated as the following:

$$Q_{pv,conv} = S_p H (T_p - T_a) \quad (4)$$

$$H = 1.2475 \left[(T_p - T_a) \cos \beta \right]^{1/3} + 2.686v \quad (5)$$

Exergy used to describe energy quality and it is the energy which can be converted to usable power. Sometimes, exergy is called available energy. In the actual process, energy conversion is irreversible. Therefore, exergy loss is also inevitable.

Exergy and exergy losses of PV modules are given in Ref. [22]:

$$E_{x,out-pv} = GS_p \left[1 - \frac{4}{3} \frac{T_a}{T_{sun}} + \frac{1}{3} \left(\frac{T_a}{T_{sun}} \right)^4 \right] - S_p \left[F_{ps} \sigma (\varepsilon_p T_p^4 - \varepsilon_s T_s^4) \right] \left(1 - \frac{T_a}{T_p} \right) - S_p H (T_p - T_a) \left(1 - \frac{T_a}{T_p} \right) - [I_{sc} V_{oc} - I_m V_m] \quad (6)$$

$$\Delta E_{pv} = (Q_{pv,rad} + Q_{pv,conv}) \left(1 - \frac{T_a}{T_p} \right) + [I_{sc} V_{oc} - I_m V_m] \quad (7)$$

The energy and exergy efficiencies of PV modules are shown:

$$\eta_{PV} = \frac{Q_{pv,elect}}{GS_p} \quad (8)$$

$$\psi_{PV} = \frac{E_{x,out-pv}}{E_{x,out-pv} + \Delta E_{pv}} \quad (9)$$

(2) Theoretical models of ISACS

(a) The compressor energy balance equation is given by:

$$\dot{m}_r h_1 + W_p = \dot{m}_r h_2 + Q_{CP,loss} \quad (10)$$

Compressor exergy model is given as:

$$\dot{m}_r [(h_1 - h_a) - T_a (s_1 - s_a)] + W_p = \dot{m}_r [(h_2 - h_a) - T_a (s_2 - s_a)] + \Delta E_{CP} \quad (11)$$

(b) The condenser energy balance equation is shown as:

$$Q_{CP,out} = \dot{m}_r h_4 + Q_a \quad (12)$$

The condenser exergy model is expressed as:

$$\dot{m}_r [(h_3 - h_a) - T_a (s_3 - s_a)] = \dot{m}_r [(h_4 - h_a) - T_a (s_4 - s_a)] + \Delta E_{CO} \quad (13)$$

(c) It is isenthalpic throttling processes to refrigerant in throttle valve, so:

$$Q_{CO,out} = Q_{TH,out} \quad (14)$$

Throttle valve exergy model is given by:

$$E_{x,out-CO} = \dot{m}_r [(h_5 - h_a) - T_a (s_5 - s_a)] + \Delta E_{TH} \quad (15)$$

(d) Evaporator energy balance equation is shown as:

$$Q_{TH,out} + Q_{AB} = Q_{CP,in} \quad (16)$$

Q_{AB} is evaporator absorption heat from water (W). Evaporator exergy model is given by:

$$\dot{m}_r [(h_5 - h_a) - T_a (s_5 - s_a)] = \dot{m}_r [(h_1 - h_a) - T_a (s_1 - s_a)] + E_{x,in-IC} + \Delta E_{EV} \quad (17)$$

The energy and exergy efficiencies of ice maker can be found as:

$$\eta_{icema} = \frac{m_{ic} \Delta h}{W_p \cdot t_{CP}} \quad (18)$$

$$\psi_{icema} = \frac{E_{x,in-IC}}{E_{x,out-pv}} \quad (19)$$

(e) Energy balance equations of air conditioning are written as:

$$m_{ic} \Delta h = C_{air} \dot{m}_{air} \Delta T_{indoor} + Q_{indoor,loss} \quad (20)$$

In thermal transfer process of ice storage conditioning, the exergy calculation is shown as:

$$E = -UA \left[T - T_{ID} - T_{ID} \ln \frac{T}{T_{ID}} \right] \quad (21)$$

The energy and exergy efficiencies of air conditioner can be found as:

$$\eta_{aircon} = \frac{C_{air} \dot{m}_{air} \Delta T_{indoor} \cdot t_{aircon}}{m_{ic} \Delta h} \quad (22)$$

$$\psi_{aircon} = \frac{E_{x,air}}{E_{x,in-IC}} \quad (23)$$

The system energy and exergy efficiencies are written as:

$$\eta = \eta_{PV} \cdot \eta_{icema} \cdot \eta_{aircon} \quad (24)$$

$$\psi = \psi_{PV} \cdot \psi_{icema} \cdot \psi_{aircon} \quad (25)$$

EXPERIMENT AND CALCULATION

The ISACS of 0.2kW driven by DPES was tested on 22th of October, in Kunming city and the irradiation q was 22.17 MJ/m² from 8:00 to 16:00. The time of ice maker operation cycle was 10 min and the ice production was about 0.35 kg every cycle. The ice making efficiency was 2.08 kg/h. The ice production is shown in Fig.2.

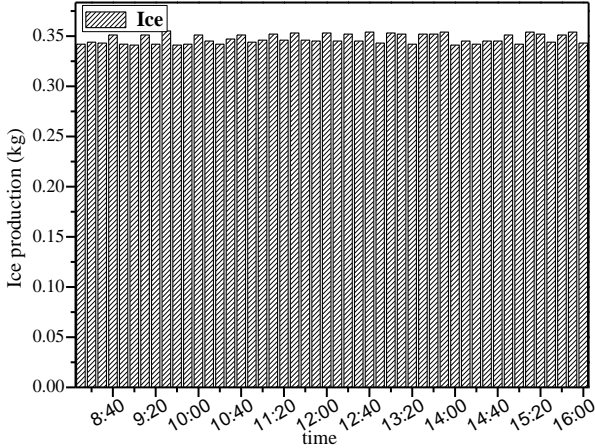


Fig.2. Ice production of ice maker

Results showed that the total amount of ice was 16.67 kg. The ice storage tank was a cube and the inside dimensions were 20 cm × 20 cm × 20 cm therefore, the volume was 0.008m³. Results revealed that the ice storage tank can supply cold for 4 hours and the changes of temperature for exchanging cold and supplying cold processes are shown in Fig.3.

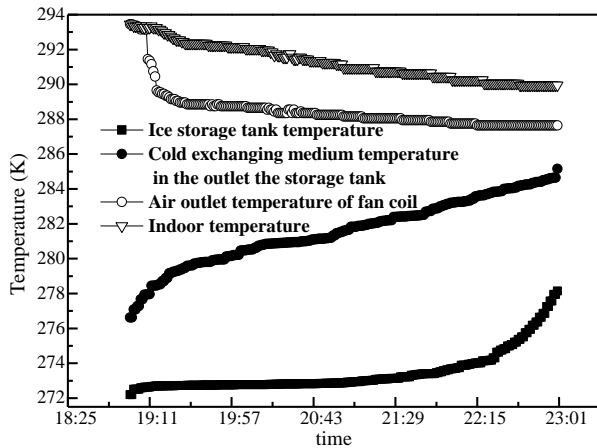


Fig.3. Temperatures change of exchanging cold and supplying cold process

The temperatures of ice maker with every component in thermodynamic cycle of ice making process have been tested in the experiment, as shown in Fig.4.

The average energy efficiency and exergy efficiencies of ISACS driven by DPES are shown

in Table 3 and the related calculation parameters are shown in Table 4.

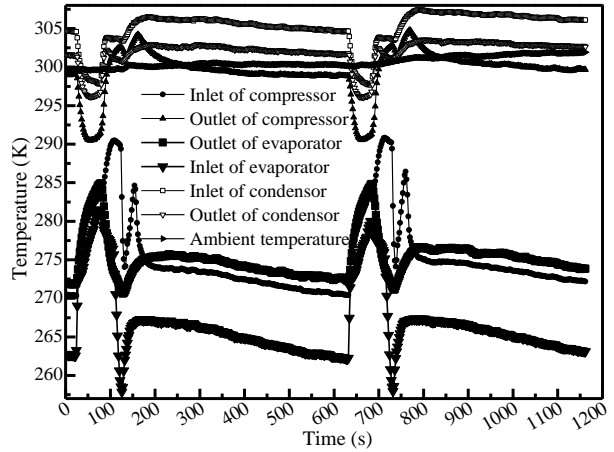


Fig.4. Temperature variations of ice maker components in thermodynamic cycle process

Table 3. Average energy and exergy efficiencies

η_{PV} /%	Ψ_{PV} /%	η_{icema} /%	Ψ_{icema} /%	η_{aircon} /%	Ψ_{aircon} /%	η /%	Ψ /%
13.30	58.84	51.31	75.02	68.00	99.99	4.64	43.91

Table 4 Related calculation parameters

Parameters	Value	Parameters	Value
Outside (08:00-16:00)		Condenser	
T_{sun}/K	5778	P_{out}/kPa	700.00
T_a/K	293.71	$h_a/(kJ\ kg^{-1})$	241.80
$v/(m\ s^{-1})$	0.78-2.52	$s_3/(kJ\ kg^{-1}\ K^{-1})$	1.7500
$q/(MJ\ m^{-2})$	22.17	$s_4/(kJ\ kg^{-1}\ K^{-1})$	1.1437
PV modules		Throttle valve	
$Q/(kW\ h)$	2.76	T_{in}/K	303.15
S_p/m^2	2.88	T_{out}/K	263.15
S_c/m^2	3.24	P_{in}/kPa	700.00
V_{OC}/V	89.35	P_{out}/kPa	200.00
I_{SC}/A	8.18	$h_a/(kJ\ kg^{-1})$	241.80
$\eta_o/\%$	17.50	$h_5/(kJ\ kg^{-1})$	395.01
α	0.92	$s_4/(kJ\ kg^{-1}\ K^{-1})$	1.1437
τ	0.90	$s_5/(kJ\ kg^{-1}\ K^{-1})$	1.7276
$m/(kg\ m^{-2})$	23	Evaporator	
T_p/K	293.71	T_{in}/K	263.15
$C_p/(J\ kg^{-1}\ K^{-1})$	1179.06	T_{out}/K	268.15
Compressor		P_{in}/kPa	200.00
$\dot{m}/(kg\ s^{-1})$	0.0127	P_{out}/kPa	243.71
W_p/W	380	$h_5/(kJ\ kg^{-1})$	241.80
T_{in}/K	268.15	$h_1/(kJ\ kg^{-1})$	395.01
T_{out}/K	313.15	$s_5/(kJ\ kg^{-1}\ K^{-1})$	1.1500
P_{in}/kPa	243.71	$s_1/(kJ\ kg^{-1}\ K^{-1})$	1.7276
P_{out}/kPa	770.21	Air conditioning	
$h_1/(kJ\ kg^{-1})$	395.01	T_{Ev}/K	263.15
$h_2/(kJ\ kg^{-1})$	425.00	T_{IC}/K	268.15
$s_1/(kJ\ kg^{-1}\ K^{-1})$	1.7276	T_{CEC}/K	278.15
$s_2/(kJ\ kg^{-1}\ K^{-1})$	1.7500	T_{FC}/K	281.15
Condenser		T_{ID}/K	293.65
T_{in}/K	313.15	$\Delta T_{indoor}/K$	0-2
T_{out}/K	303.15	$UA/(W\ K^{-1})$	22.738
P_{in}/kPa	700.00	$C_{air}/(kJ\ kg^{-1}\ K^{-1})$	1
$h_3/(kJ\ kg^{-1})$	425.00	$\dot{m}_{air}/(kg\ s^{-1})$	0.12

RESULTS AND DISCUSSION

From the calculation results, it was found that system energy efficiency was only 4.64% at most of energy losses in ice making process. In the ice making process, ice pasted well together with a five solid walls of grid plate evaporator and cannot be separated off by ice gravity. Thus, the compressor must be shut down and a special solenoid valve must be opened which used for adjust refrigerant flow and introduced the high temperature and high pressure refrigerant steam expelled from compressor into evaporator. And then, the evaporator plays the role of condenser to release the evaporator plays the role of condenser to release heat to ice through solid walls and ice interfaces begin melting. The ice temperature increased and was stripped off evaporator and fall into ice storage tank. Meanwhile, evaporator inlet and outlet temperatures increased sharply until the solenoid valve closed and the compressor was turned on and a new ice making process begins. The refrigerant flowed out of evaporator into throttle valve at a low temperature and low pressure liquid. And then, the refrigerant flow into condenser to absorb heat from outside and the condenser inlet and outlet temperatures decline sharply when the low temperature refrigerant flows into it. It was observed that the condenser outlet temperature was higher than the condenser inlet temperature because refrigerant can absorb heat from the outside of the condenser, as shown in Fig. 4. Then, the refrigerant flow into the compressor

and the compressor inlet temperature increased compared to the ice making process. The temperature of refrigerant can be changed with the variation of inlet and outlet temperatures of the evaporator and condenser. The compressor stop running in ice melting abscission process and the refrigerant gas cannot be compressed in compressor. Therefore, the compressor outlet dropped sharply when the solenoid valve opens and it returns smoothly when ice making process started. Ice melting abscission process was extremely unfavourable for the system energy utilization for two reasons as the following:

a) The cold consumption was high and the ice temperature increased from 268.15K to 270.15K in ice melting abscission process;

b) The ice maker operation period was extended for 200s; furthermore, the ice melting abscission time was one third of the ice making cycle.

System optimization

Therefore, in order to improve the performance of ISACS driven by DPES and promote the project commercial promotion, the structure optimization measurement of ice maker were proposed as the following:

a) Evaporator immersion static refrigeration mode was adopted to replace ice harvester refrigeration mode. Moreover, the optimized coil evaporator was immersed into water to absorb heat and then the water could be frozen on the evaporator. Thus, most of the energy could be utilized. The structure diagram is shown in Fig.5.

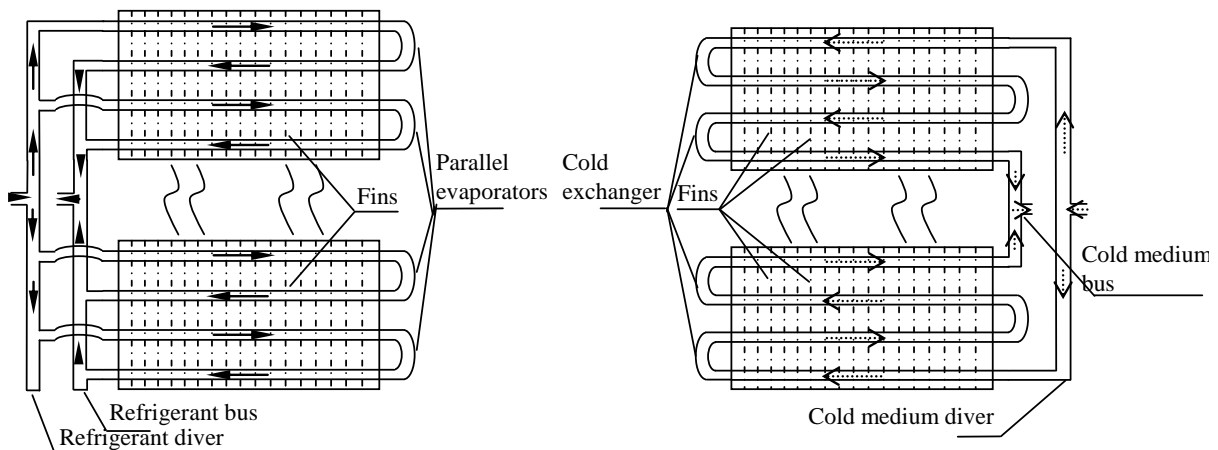


Fig.5. Profile of evaporators and cold exchanger immersed in the ice storage tank

b) The coil cold exchanger was co-integrated with coil evaporator. In the refrigeration process, coil cold exchanger has the priority to get cold by

the transferred heat from the coil evaporator to supply cold for user and the surplus cold could be used to make ice. So, the energy could be stored in

ice. Consequently, ISACS not only has the out-of-the-box function of ordinary air conditioning, but also effectively improve the appearing phenomenon of over cooling and remedy the disadvantage of cold supply after the ice making process in the

traditional submerged ice making system. The top view of co-integration evaporators and cold exchanger immersed in the ice storage tank is shown in Fig.6.

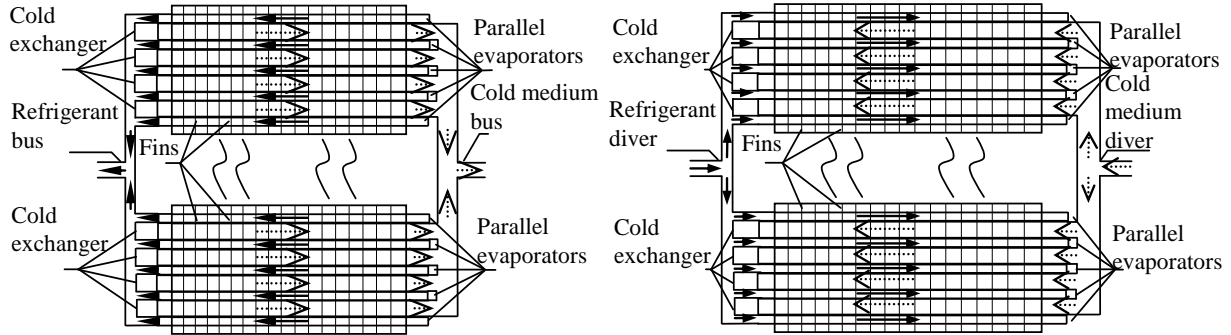


Fig.6. Top view of co-integration evaporators and cold exchanger immersed in the ice storage tank

The performance of optimized ISACS driven by DPES can be simulated as mentioned above. After the optimization, it was observed that the energy efficiency could be improved from 51.31% to 75.02% and the exergy efficiency could be improved from 90% to 97.45% in ice making process. The system energy efficiency increased from 4.64% to 8.14% and the system exergy efficiency increased from 43.91% to 57.33%.

CONCLUSION

1. The energy characteristics and the simulation analysis of ISACS driven by DPES were carried out as well as the experimental platform was built to verify the theoretical model. Results showed that energy utilization ratio and exergy efficiency were 4.64% and 43.91%, respectively. The photoelectric conversion efficiency of PV modules was 13.28% at 58.83% exergy efficiency and the ice maker COP was 51.31% at 75.02% exergy efficiency. Most of the energy was consumed in the photoelectric converting process in PV modules and refrigeration process with ice maker. It was a hard work to improve the photoelectric conversion efficiency of PV modules. So, the optimization design for the ice maker model should be carried out.

2. The evaporator immersion static refrigeration mode was adopted to replace the ice harvester refrigeration mode to achieve high efficiency refrigeration. Meanwhile, coil cold exchanger was co-integrated with coil evaporator.

3. The energy efficiency of the optimized ice maker could be increased from 51.31% to 75.02% and the exergy efficiency could be improved from 90% to 97.45%, respectively.

ACKNOWLEDGEMENTS

The authors gratefully acknowledge the financial support provided by National International Scientific and Technological Cooperation Program (2011DFA62380). The authors are also grateful to Renewable Energy Research and Innovation Development Center in Southwest China (05300205020516009), Research and Innovation Team of Renewable Energy in Yunnan Province and Yunnan Provincial Renewable Energy Engineer Key Laboratory (2015KF05) and Yunnan Provincial Department of Education Science Research Fund Project (2015J035).

NOMENCLATURE

Roman symbols			
		1	refrigerant in state 1
C	specific heat capacity ($J\ kg^{-1}\ K^{-1}$)	2	refrigerant in state 2
ΔE	exergy loss (W)	3	refrigerant in state 3
E_x	exergy (W)	4	refrigerant in state 4
F_{ps}	panel to sky view factor, 1	5	refrigerant in state 5
G	solar irradiance ($W\ m^{-2}$)	a	ambient
h	enthalpy ($J\ kg^{-1}$)	air	indoor air
I	current (A)	$aircon$	air conditioning
m	PV module mass per square meter ($kg\ m^{-2}$)	c	cell
\dot{m}	mass flow ($kg\ s^{-1}$)	$conv$	convective
Q	power per unit time (W)	CP	compressor
Q_{AB}	evaporator absorption heat from water per unit time (W)	CO	condenser
S	area(m^2)	$elect$	electricity
s	entropy ($J\ kg^{-1}\ K^{-1}$)	in	input
t	runtime (s)	IC	ice
T	temperature (K)	ID	indoor
V	voltage (V)	$loss$	loss

UA	Heat transfer resistance ($W K^{-1}$)	m	maximum power point
v	speed ($m s^{-1}$)	oc	open circuit
W_p	compressor operating power (W)	out	output
<i>Greek symbols</i>		p	parallel
α	Solar cell absorption coefficient	pv	PV modules
β	PV modules tilt angle ($^\circ$)	r	reference
τ	PV module cover glass transmittance	rad	radiation
σ	Stephan-Boltzmann constant ($5.76 \times 10^{-8} W m^{-2} K^{-4}$)	s	sky
ε_p	the average emissivity of PV modules, 0.8	sc	Short-circuit
ε_s	average emissivity of sky, 1		
η	average energy efficiency	sun	sun
ψ	average exergy efficiency	TH	Throttle valve
<i>Subscripts</i>			
0	reverse saturation		

REFERENCES

- 1 Allouhi A, Kousksou T, Jamil A, Bruel P, Mourad Y, Zeraouli Y, *Renew Sustain Energy Rev*, 44, 159 (2015).
- 2 Ghafoor A, Munir A, *Renew Sustain Energy Rev*, 43, 763, (2015).
- 3 Khattab NM, Sharawy H, Helmy M, *Energy Procedia*, 18, 709, (2012).
- 4 Attan D, Alghoul MA, Saha BB, Assadeq J, Sopian K, *Renew Sustain Energy Rev*, 15, 1708, (2011).
- 5 Du S, Wang RZ, Xia ZZ, *Energy*, 80, 687, (2015).
- 6 Pan QW, Wang RZ, Lu ZS, Wang LW, *Appl Therm Eng*, 72, 275, (2014).
- 7 Xu ZY, Wang RZ, *Energy*, 77, 703 (2014).
- 8 Du S, Wang RZ, Xia ZZ, *Energy*, 68, 862, (2014).
- 9 Jiang L, Wang LW, Wang RZ, *Int J Therm Sci*, 81, 68, (2014).
- 10 Ji X, Li M, Fan J, Zhang P, Luo B, Wang L, *Appl Energy*, 113, 1293, (2014).
- 11 Xu Ji, Xiangbo Song, Ming Li, Jiaying Liu, Yunfeng Wang, *Energy Convers Manag*, 106, 759, (2015).
- 12 Axaopoulos PJ, Theodoridis MP, *Sol Energy*, 83, 1360, (2009).
- 13 Bilgili M, *Sol Energy*, 85, 2720, (2011).
- 14 Ekren O, Yilanci A, Cetin E, Ozturk HK, *IEEE Elektronika ir elektrotechnika*, 114, 7, (2011).
- 15 Aktacir M A, *Int J Phys Sci*, 6, 746, (2011).
- 16 Mba EF, Chukwunke J L, Achebe C H, *J Info Eng App*, 2, 1, (2012).
- 17 Tina GM, Grasso AD, *Energ Convers Manag*, 78, 862, (2014).
- 18 Kaplanis S, Papanastasiou N, *Renew Energ*, 31, 771, (2006).
- 19 Modi A, Chaudhuri A, Vijay B, Mathur J, *Appl Energ*, 86, 2583, (2009).
- 20 Li Y, Zhou SH, Lin WD, Ji X, Luo X, Li M, *Acta Energ Sol Sinica*, 36, 422, (2015).
- 21 Rabl A, USA: *Oxford University Press* 1985.
- 22 Ekren O, Celik S, Noble B, Krauss R, *Int J Refrig*, 36, 745, (2013).